THE COVARIABILITY BETWEEN ANOMALOUS NORTHEAST MONSOON RAINFALL IN MALAYSIA AND SEA SURFACE TEMPERATURE IN INDIAN-PACIFIC SECTOR: A SINGULAR VALUE DECOMPOSITION ANALYSIS APPROACH

Liew Juneng and Fredolin T. Tangang*

Marine Science Program, School of Environmental and Natural Resources Science,
Faculty of Science and Technology, Universiti Kebangsaan Malaysia,
43000 Bangi, Selangor, Malaysia

*Corresponding author: tangang@pkrisc.cc.ukm.my

Abstract: *The singular value decomposition technique (SVD) is used to analyze the covariability between anomalous northeast monsoon (NEM) rainfall in Malaysia and the large-scale anomalous sea surface temperature (SST) in Indian Ocean, Pacific Ocean and seas surrounding the Maritime Continent. The SVD analysis reveals two significant coupled modes of covariability with the first dominant mode explaining ~75% while the second coupled mode explaining ~15% of the total covariance. The first coupled mode highlights the covariability between anomalous NEM rainfall in East Malaysia and anomalous SST associated with the biennial oscillation type (BO-type) of the El Nino-Southern Oscillation (ENSO). The second coupled mode highlights the covariability between anomalous NEM rainfall in West Malaysia and anomalous SST associated with the low frequency type (LF-type) of ENSO. Overall, the BO-type and LF-type of ENSO define two distinct regimes of different behaviour of anomalous NEM rainfall in Malaysia East Malaysia and West Malaysia regions. During the BO-type of ENSO, East Malaysia region is mostly affected while during the LF-type of ENSO, the impacts are mostly confined in West Malaysia region.*

Keywords: singular value decomposition, covariability, northeast monsoon rainfall, sea surface temperature

1. INTRODUCTION

The singular value decomposition (SVD) is a commonly used technique in meteorological and oceanographic data analysis [1–4]. It can be thought of as a generalization to the square symmetric matrix diagonalization technique such as the empirical orthogonal function (EOF) analysis. However, unlike the EOF which is used to decompose a space and time distributed data matrix of a single field (e.g., Tangang [5]), the SVD technique is applied to two data matrices of two jointly analyzed fields to identify pairs of the coupled spatial pattern and their respective temporal variations. Each pair explains a fraction of covariance between the two jointly analyzed fields. This decomposition allows the extraction of dominant modes of coupled covariability between the two analyzed fields.

This is important since the dominant modes of covariance are often amenable to physical interpretation and usually led to an insight into the complex processes responsible in modulating the covariability. The technique is also useful because of its applicability to both regularly or irregularly gridded datasets.

In this paper, the SVD technique is used to analyze the covariability between the anomalous northeast monsoon (NEM) rainfall anomaly in Malaysia and the large-scale sea surface temperature (SST) anomaly in Indian Ocean, Pacific Ocean and surrounding seas in the Maritime Continent. The relationship between anomalous rainfall in Malaysia and the anomalous SST has been investigated in previous studies [5–9]. However, most analyses were based on the EOF analyses that highlighted individual rather than coupled modes. In general, the interannual variability of anomalous rainfall in Malaysia can be partially explained by the anomalous SST associated with El Nino Southern Oscillation (ENSO) event. Tangang and Juneng [8] shows that the interannual variability of Malaysian rainfall associated with ENSO events peaks during the NEM period. However, the strong ENSO-Malaysian rainfall relationship during the NEM period is only apparent in East Malaysia [9]. Juneng and Tangang [9] attributed this to the seasonal migration of ENSO signal in the region associated with the remote forcing and ocean-atmosphere interaction in the region. This seasonal migration of ENSO signal represents the most dominant mode of variability of anomalous rainfall in Malaysia. In this study, we employ the SVD technique to address two questions. First, does the individual dominant mode in anomalous rainfall in Malaysia during NEM period represents dominant coupled mode variability? Second, why do the anomalous rainfalls in West Malaysia and East Malaysia behave differently? Could these different behaviours be attributed to two different couple modes?

2. THE PRINCIPLE OF SVD TECHNIQUE

In order to perform the SVD technique jointly on two space-time distributed data fields, the temporal cross-covariance matrix between the two data fields needs to be computed. The number of stations or grids in each data field may not necessary be equal. However, the technique requires that the two data fields span an identical temporal period. Assume S and P are the analyzed data field with dimension $M_s \times N$ and $M_p \times N$, respectively. The M_s and M_p indicate the spatial grid points of S and P, respectively, while N represents the identical temporal points of both S and P. The temporal cross-covariance matrix can be constructed as:

$$\mathrm{C} = SP^T = \begin{pmatrix} S_1P_1 & S_1P_2 & \cdots & S_1P_{M_P} \\ S_2P_1 & S_2P_2 & \cdots & S_2P_{M_P} \\ \vdots & \vdots & & \vdots \\ S_{M_S}P_1 & S_{M_S}P_2 & \cdots & S_{M_S}P_{M_P} \end{pmatrix} \quad (1)$$

with each element of the matrix, $\langle S_iP_j \rangle$, corresponds to the spatial cross-covariance between the time series S_i and P_j at grids i and j, respectively. Based on the cross-covariance matrix, C, matrices U, V and L can be computed such that:

$$C = ULV^T \quad (2)$$

The singular vectors for S are given by the columns of U (often called the *left pattern*) while that corresponding singular vectors for P are given by the columns of V (*right pattern*). U and V are both orthogonal while L is a diagonal matrix whose dimension is of $M_s \times M_p$. The diagonal elements of matrix L are referred as the singular values. The total squared covariance can be computed by taking the summation of all the squared singular values of diagonal elements of L. The maximum number of non-zero singular values (defined as the number of SVD modes) of the decomposition is $\kappa = \min(M_s, M_p)$. The expansion coefficients, which describe the time variability in each mode, can now be obtained by projecting each field onto their respective singular vectors. For field S, the expansion coefficients can be computed as:

$$A_s = SU \quad (3)$$

while the corresponding expansion coefficients for P are given as:

$$A_p = PV \quad (4)$$

The k-th column of the matrices A_s and A_p contains the expansion coefficients for k-th SVD mode for field S and P, respectively. Since both U and V are orthogonal, the original field can be easily reconstructed using the relationship:

$$S = A_sU^T \quad (5)$$

and

$$P = A_pV^T \quad (6)$$

The relative importance of each SVD mode is indicated by the percentage of squared covariance (PSC) for that associated SVD mode. The k-th mode PSC is given as:

$$\mathrm{PSC}_k = \frac{l_k}{\sum_{i=1}^{\kappa} l_i} \tag{7}$$

where l_k is the k-th diagonal elements of L. Only significant modes of covariability will be retained for further analysis and interpretation. For each SVD mode of covariability between S and P, two analysis products will be scrutinized – a pair of the homogenous maps and a pair of expansion coefficient time series (called temporal amplitude). The homogenous map is obtained by correlating the temporal amplitude with its respective data field. The homogenous map displays the spatial pattern of coupled mode in each data field while the temporal amplitude characterizes its temporal evolution. A detail mathematical treatment of SVD technique can be found in Bretherton et al. [1].

3. DATA AND METHOD

The rainfall data used in the study was obtained from Global Historical Climatology Network (GHCN) and Malaysia Meteorological Department (MMD). The GHCN data is based on the data exchanged from the World Meteorological Organization (WMO) as part of the World Weather Watch Program [10]. A total of 14 stations were considered in this study (Fig. 1). The selection of these stations was based on the geographical distribution as well as the availability of the dataset. In some of the stations, the GHCN data extended back to the late 1800s, with some periods of missing values. However, in this study we only considered rainfall data that spans a period of nearly 50 years from January 1951 to May 2000. The SST data in $1^o \times 1^o$ resolution used in the study was the version 1.1 of Hadley Center Global Ice and Sea Surface Temperature (HADiSST1) obtained from the United Kingdom Meteorological Office (UKMO) [11]. For computational efficiency, the gridded SST were averaged into coarser grids of 2° × 2°. Together with the SST, 850 hPa wind (UV850) of National Center of Environmental Prediction (NCEP) reanalysis from Climate Diagnostic Center (CDC) was also used [12]. The UV850 was the interpolated to 5° × 5° grids from the original resolution of 2.5° × 2.5°.

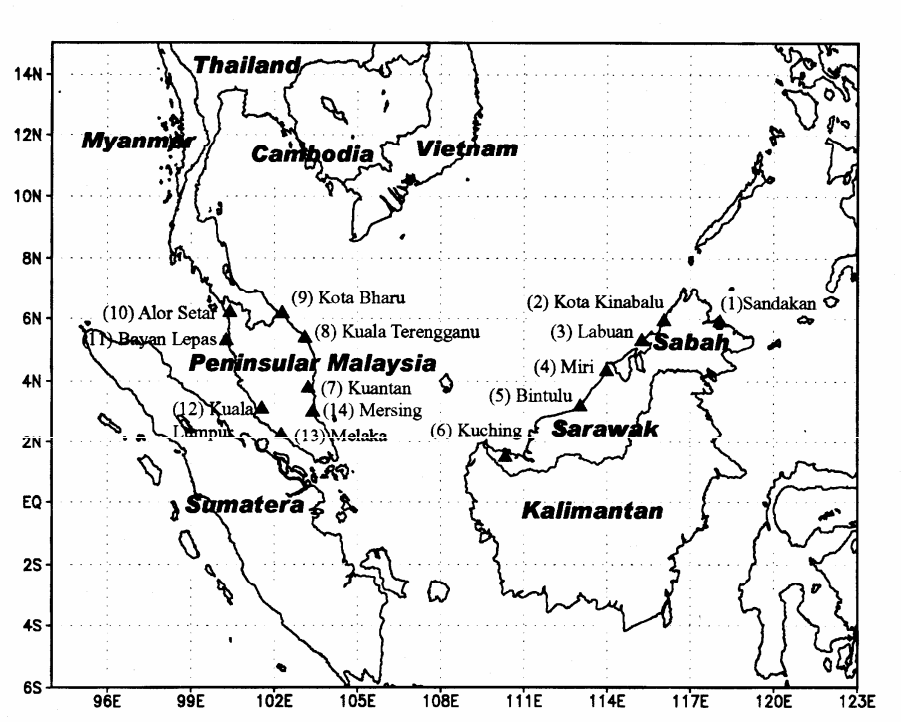

Figure 1: The location of the 14 stations used in this study, with numbers in parenthesis representing station numbers to be used in subsequent figures.

We defined the NEM period to cover a period of four months from November to February the following year. Prior to the analysis, all anomalous data fields were standardized according to Arthur and Jagtap [13] and computed as:

$$A_{it} = \frac{X_{it} - \bar{X}_i}{SD_i} \tag{8}$$

where

A_{it} is the standardized anomalies at year t and grid or station i,

X_{it} is the averaged data value for November (0)–February (1) at year t and grid or station i,

$\bar{X}_i$ is the climatology value from 1951–1999 at grid or station i, and

SD_i is the standard deviation of the time series at station i.

For convenience, the rainfall time series in each station are arranged in the rows of the data matrix according to the station numbers shown in Figure 1. The standardized anomalous rainfall and SST data were then subjected to the SVD analysis.

4. RESULTS AND DISCUSSION

The number of SVD modes corresponds to the station number (i.e., the minimum between the number of rainfall stations and SST grids). Figure 2 displays the PSC values for each of the 14 SVD modes. Also shown is the 95% significant level estimated using a Monte Carlo randomization experiment [4,14]. The first mode of covariability, that accounts for more than 75% of PSC, dominates the covariability between the two fields. The second mode, which accounts to ~15% of PSC, is also significant. The subsequent modes account for insignificant portion of the PSC. Only the first two SVD modes are subjected to further discussion.

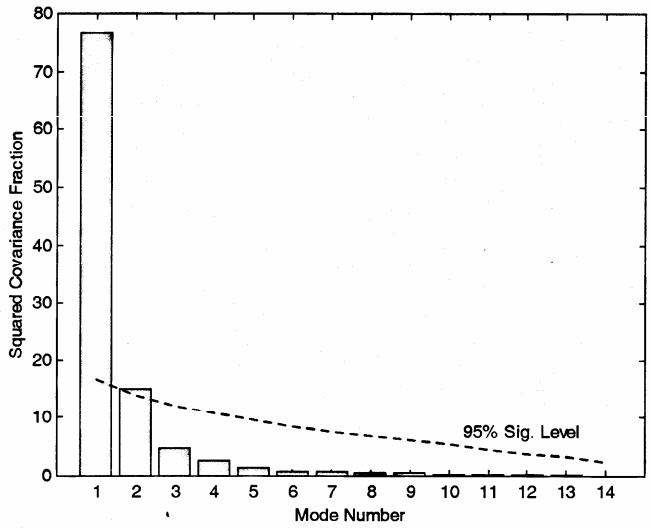

Figure 2: The percentage of squared covariance for each of the 14 coupled modes. The dotted lines indicate 95% confidence limit

The homogeneous map of the first dominant mode associated with the anomalous NEM rainfall is shown in Figure 3(a). The pattern shows concentration of higher loadings on the stations located in East Malaysia (except Kuching) with loading values of ~0.9. Kuching station, which is located at western side of Borneo, displays only a weak loading value of ~0.2. There is a

clear distinction between stations in East and West Malaysia as the stations in West Malaysia display relatively weak loadings of ~0.3. The corresponding SST homogeneous map of mode 1 [Figure 3(b)] resembles the typical pattern of anomalous SST during the peak of a cold ENSO episode (i.e., La Nina) with negative anomalies covering the eastern-central Pacific and a basin wide cooling in the Indian Ocean and seas surrounding the Maritime Continent (e.g., Rasmusson and Carpenter [15]). These spatial patterns in rainfall and SST represent the dominant coupled modes between NEM anomalous rainfall and anomalous SST in Indian-Pacific sector. Indeed, the temporal amplitude for rainfall and the southern oscillation index (SOI) correlate each other very well (~0.88), indicating the coupled nature of the phenomenon (Fig. 4). This association indicates that in conjunction with a La Nina event, East Malaysia region will experience anomalous high NEM rainfall. Likewise, assuming a linear polarity of ENSO, during an El Nino event, the region will experience anomalously low NEM rainfall.

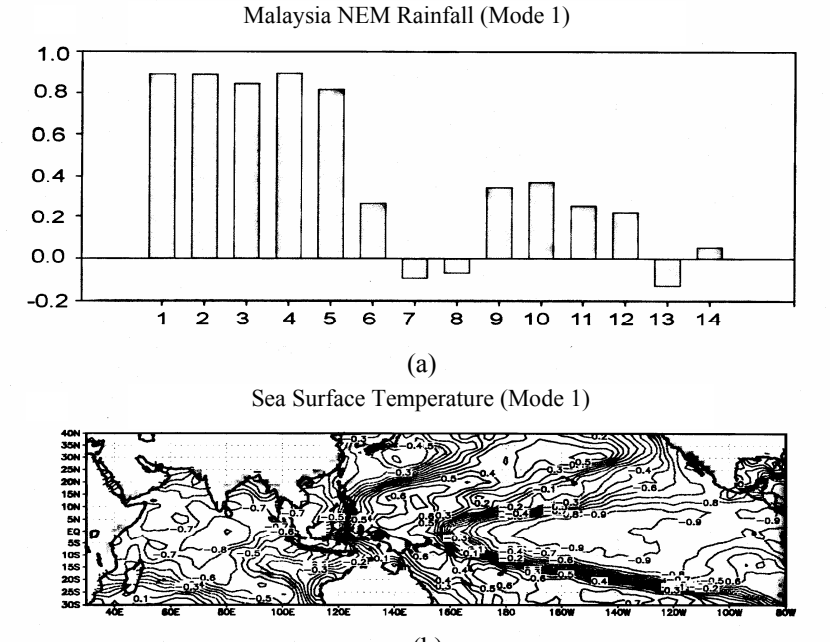

Figure 3: The homogenous maps for the first dominant coupled mode, (a) anomalous rainfall pattern, and (b) anomalous SST pattern

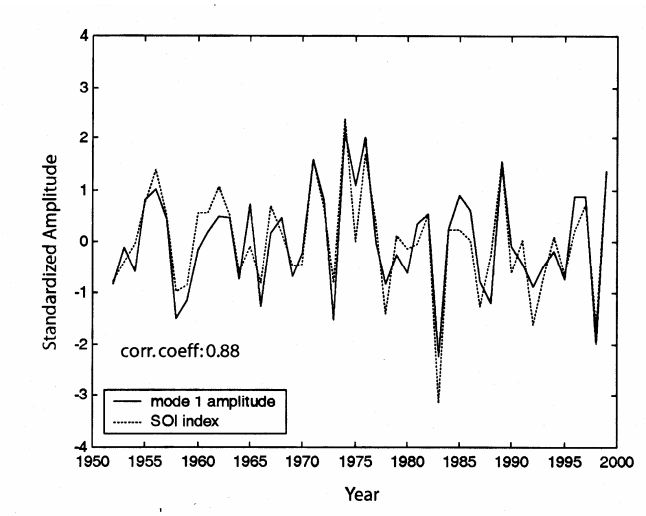

Figure 4: The temporal amplitude of anomalous rainfall for the first dominant coupled mode. Also shown is the SOI

These results are consistent with those presented in Tangang and Juneng [8] and Juneng and Tangang [9]. Tangang and Juneng [8], through composite analysis of wet-dry events showed that the anomalous SST pattern as shown in Figure 3(b) is associated with anomalous rainfall in Malaysia. However, Tangang and Juneng [8] did not specifically associate the anomalous SST pattern with the anomalous rainfall in East Malaysia since the index used was a single rainfall index to represent the whole Malaysian region. However, Figure 3(a) clearly indicates that the anomalous SST pattern couples to the anomalous rainfall in East Malaysia. This is consistent with Juneng and Tangang [9], that showed the ENSO coherence in anomalous rainfall resides over northern Borneo during the NEM period. Juneng and Tangang [9] argued that the anomalous rainfall over northern Borneo and southern Philippines is due to the strengthening of the anomalous cyclonic/anti-cyclonic circulation over the western North Pacific (WNP) region. Indeed, the correlation pattern between mode 1 temporal amplitudes and both u and v components of the 850 hPa anomalous wind indicates the same anomalous circulation over the WNP region (Fig. 5). The strengthening of this anomalous circulation is very much related to the strengthening of an SST dipole in the WNP region [9]. In Figure 3(a), the sign of anomalous SST in the South China Sea (SCS) and seas around Japan is opposite to that in region east of Philippines, creating a very strong SST gradient in the WNP region. Juneng and Tangang [9] argued that the anomalous circulation is actually responsible transporting anomalous moisture into the region during the peak of a La Nina event. The scenario reverses during an El Nino event. However, the influences of this anomalous circulation confine in northern Borneo and southern Philippines without significantly affecting West Malaysia, southern

Borneo and Indonesian region south of Borneo. Hendon [16] noted that the ENSO-Indonesian rainfall coherence diminishes during this period. Interestingly, the dominant coupled mode shows a biennial tendency with a preferred periodicity of 2 to 2.5 years (Fig. 6). This is a strong indication that the anomalous rainfall during NEM period in East Malaysia is modulated by ENSO of biennial type.

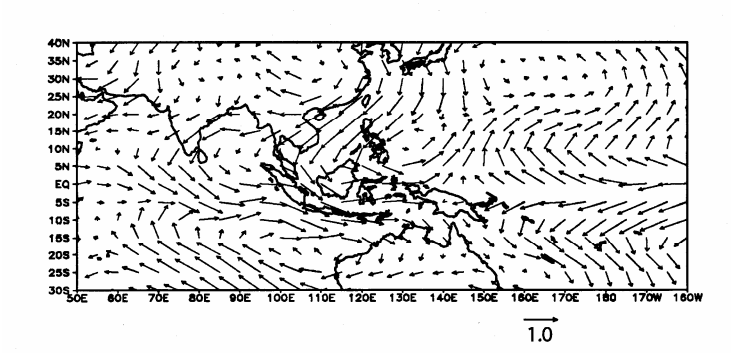

Figure 5: The correlation vectors between the temporal amplitudes of the first coupled mode and the *u* and *v* component of anomalous 850 hPa wind

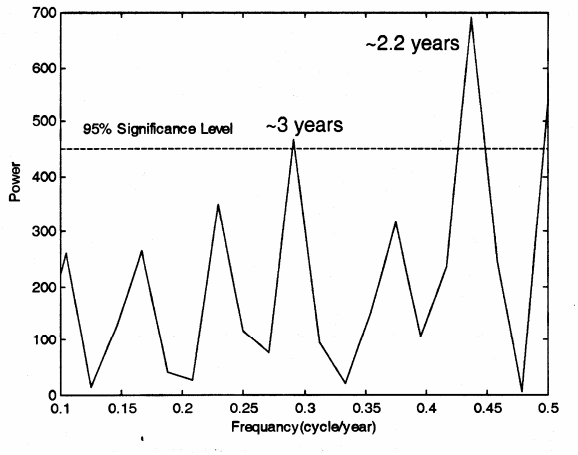

Figure 6: The spectrum of the temporal amplitude of the first coupled mode

The first dominant coupled mode is dominated by the covariability of East Malaysian NEM rainfall and the SST. However, the second coupled mode is dominated by covariability between West Malaysian rainfall and the SST (Fig. 7). The explained portion of the PSC is relatively low (i.e., ~15%) compared to the first mode (Fig. 2). This implies the covariability of anomalous rainfall in Malaysia and anomalous SST during NEM is dominated by the

covariability in East Malaysia. The homogenous maps for both anomalous NEM rainfall and SST of the second mode clearly show different patterns than that of the first mode. The rainfall pattern shows concentration of significantly higher loadings in West Malaysian stations [Fig. 7(a)]. The associated pattern for the SST shows a quite different scenario than that of a typical ENSO event [Fig. 7(b)] indicating a different phenomenon modulating this coupled mode.

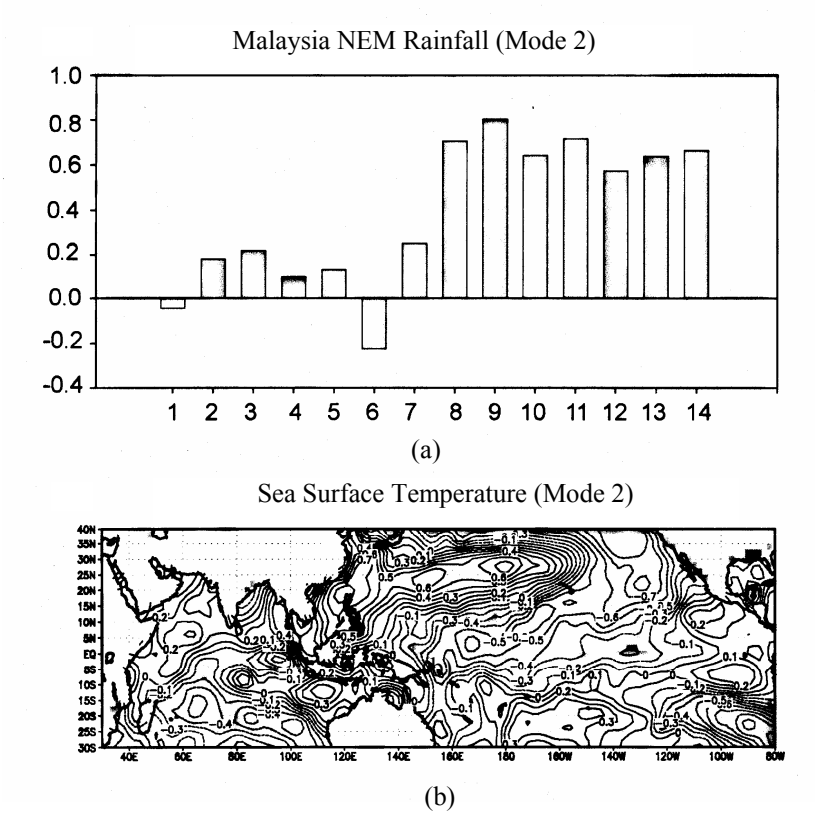

Figure 7: As in Figure 3 except for the second dominant coupled mode

Indeed, the phenomenon must be distinct to the typical biennial type of ENSO as the temporal amplitude of this second coupled mode does not correlate significantly with the SOI (Fig. 8). Figure 8 also stresses that the two phenomena modulating the anomalous NEM rainfall in East and West Malaysia are distinct and occur at different times. In fact, the characteristic of the temporal amplitudes seems to indicate a shift with higher (lower) frequency of oscillation before (after) 1970s. Overall the periodicity of this second coupled mode covers between 4 to 6 years (Fig. 10). The periodicity seems to suggest that the phenomenon modulating this coupled mode may be related to the so-called low frequency ENSO type. Also, the correlation between the temporal amplitudes and

the *u* and *v* components of anomalous 850 hPa winds indicate a weaker anomalous cyclonic circulation (Fig. 9). Compared to Figure 5, this anomalous circulation is shifted westward to be over the Peninsular Malaysia.

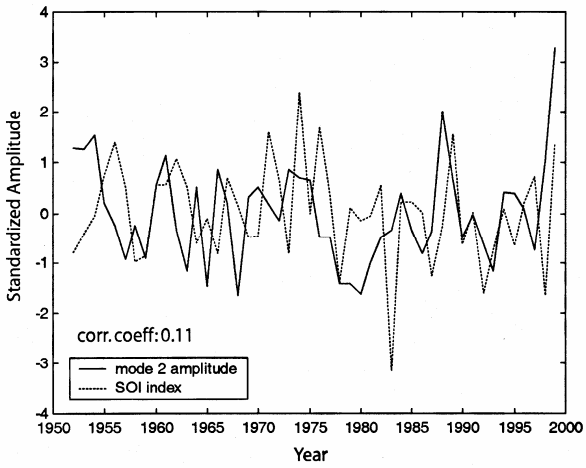

Figure 8: As in Figure 4 except for the second dominant coupled mode

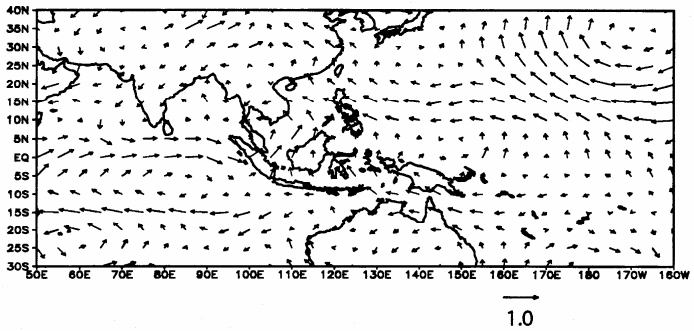

Figure 9: As in Figure 5 except for the second dominant coupled mode

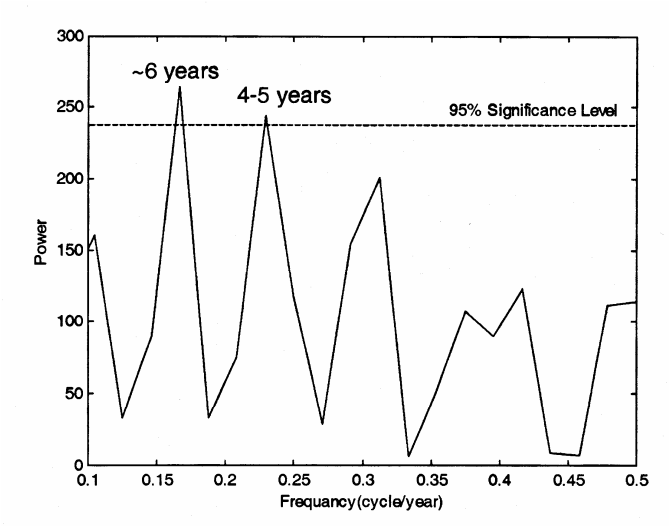

Figure 10: As in Figure 6 except for the second dominant coupled mode

The SVD analysis identifies two coupled modes of distinct characteristics. The covariability in the anomalous NEM rainfall – SST data is dominated by the covariability in East Malaysia with ~75% of the PSC while the covariability in West Malaysia shows a much lower but significant portion of the PSC (i.e., ~15%). These two modes of covariability highlight two regimes of different anomalous NEM rainfall behaviour in Malaysia. Both phenomena modulating these two dominant covariability modes are obviously distinct. The interesting question to investigate is whether these phenomena correspond to the two types of ENSO – the biennial type of ENSO (BO-type) and the low frequency type of ENSO (LF-type). The classification of ENSO types has been a subject of numerous investigations [17–21]. Barnett [19] classified ENSO events into three categories of intensity based on the inter-phase relationship and amplitude component of ENSO fluctuation in period of 20–30 months (BO-type) as well as 40–60 months (LF-type). Tomita and Yasunari [20] classified ENSO into two categories based on the lasting period of the events. Events that end within a year time are categorized as BO- type while those last about two years categorized as LF-type of ENSO. Ose et al. [21] introduced a different classification scheme based solely on the signs of SST anomaly in the eastern-central Pacific Ocean and SCS. When the signs of SST anomaly in both SCS and central Pacific are identical, the event is categorized as BO-type while it is categorized as LF-type if the polarities are out of phase. The anomalous SST pattern associated with the first dominant coupled mode indicates in-phase SST anomalies in eastern-central Pacific Ocean and SCS [Fig. 3(b)]. The corresponding pattern for the second coupled mode indicates opposite polarity of SST anomaly in the two regions [Fig. 7(b)]. Adopting Ose et al. [21] classification scheme, Figures 3(b) and 7(b) support our earlier contention that the coupled modes in East and West Malaysia

are modulated by the BO-type of ENSO and the LF-type of ENSO, respectively. Indeed for the first coupled mode, the SST anomalous pattern [Fig. 3(b)] and the position of the anomalous circulation (Fig. 5) are consistent with the corresponding BO-type patterns in Ose et al. [21]. Likewise, the SST anomalous pattern [Fig. 7(b)] and the anomalous circulation (Fig. 9) for the second coupled mode are similar to that of the LF-type in Ose et al. [21]. During a BO-type of ENSO, the anomalous SST conditions in the WNP region sustain the anomalous circulation in the region. The anomalous circulation in turn brings the moisture into (out of) the region resulting in anomalously high (low) rainfall during the NEM period in East Malaysia. During the LF-type, the anomalous SST pattern changes resulting in weaker anomalous circulation with its centre shifted to be over West Malaysia.

5. CONCLUSION

The SVD analysis on the anomalous NEM rainfall and anomalous SST in the Indian-Pacific sector reveals two dominant coupled modes. The first coupled mode that dominates the covariability between the anomalous NEM rainfall and the SST reveals the covariability between anomalous NEM rainfall in East Malaysia and anomalous SST associated with the BO-type of ENSO. The atmosphere-ocean interaction in the WNP region during the NEM period sustains the anomalous cyclonic (anti-cyclonic) circulation over the region. The anomalous circulation in turn provides the mechanism for anomalous moisture convergence (divergence) into southern Philippines and northern Borneo. The second coupled mode highlights the covariability between the anomalous NEM rainfall in West Malaysia and anomalous SST associated with the LF-type of ENSO. The anomalous circulation associated with this anomalous SST shifted westward with its centre located over West Malaysia. Overall, the SVD analysis reveals two types of ENSO (i.e., the BO-type and LF-type) that define two distinct anomalous NEM rainfall regimes in Malaysia. During the BO-type of ENSO, the East Malaysia region is mostly affected. On the other hand, during the LF-type of ENSO the impacts are mostly confined in West Malaysia region.

6. ACKNOWLEDGEMENTS

The authors are grateful to various agencies – MMD, UKMO, CDC-NCEP for providing various datasets. This research was funded by the Malaysian Ministry of Science, Technology and Innovation (MOSTI) IRPA grant 08-02-02-0012-EA215.

7. REFERENCES

1. Bretherton, C.S., Smith, C. & Wallace, J.M. (1992). An intercomparison of methods for finding couples patterns in climate data. *Journal of Climate*, 5, 541–560.
2. Wallace, J.M., Smith, C. & Bretherton, C.S. (1992). Singular value decomposition of wintertime sea surface temperature and 500-mb height anomalies. *Journal of Climate*, 5, 561–576.
3. Cherry, S. (1996). Singular value decomposition analysis and canonical correlation analysis. *Journal of Climate*, 9, 2003–2009.
4. Venegas, S., Mysak, L. & Straub, D. (1996). Evidence for interannual and interdecadal climate variability in the South Atlantic. *Geophysical Research Letters*, 23(19), 2673–2676.
5. Tangang, F.T. (1999). Empirical orthogonal function analysis of precipitation anomaly in Malaysia. *Malaysian Journal of Analytical Sciences*, 5, 155–165.
6. Tangang, F.T. (2001). The quasi-biennial and low-frequency oscillation in the Malaysian precipitation anomaly. *International Journal of Climatology*, 21(10), 1199–1210.
7. Juneng, L. & Tangang, F.T. (2003). Malaysia monsoon rainfall variability and its predictability in relation to large-scale forcing. *Sains Malaysiana*, 32(2), 1–13.
8. Tangang, F.T. & Juneng, L. (2004). Mechanism of Malaysian rainfall anomalies. *Journal of Climate*, 17(18), 3615–3621.
9. Juneng, L. & Tangang, F.T. (2005). Evolution of ENSO-related rainfall anomalies in Southeast Asia region and its relationship with atmosphere-ocean variations in Indo-Pacific sector. *Climate Dynamic*, 25(4), 337–350.
10. Vose, R.S., Schmoyer, R.L., Steurer, P.M., Peterson, T.C., Heim, R., Karl, T.R. & Eischeid, J. (1992). *The Global Historical Climatology Network: Long-term monthly temperature, precipitation, sea level pressure, and station pressure data.* ORNL/CDIAC-53, NDP-041. Oak Ridge, Tennessee: Carbon Dioxide Information Analysis Center, Oak Ridge National Laboratory.
11. Rayner, N.A., Parker, D.E., Horton, E.B., Forland, C.K., Alaxender, L.V., Rowel, D.P., Kent, E.C. & Kaplan, A. (2003). Global analyses of SST, sea ice and night marine air temperature since the late nineteenth century. *Journal of Geophysical Research*, 108(D14), 4407, DOI: 10.1029/2002JD002670.
12. Kalnay, E., Kanamitsu, M., Kistler, R., Collins, W., Deaven, D., Gandin, L., Iredell, M., Saha, S., White, G., Woolen, J., Zhu, Y., Chelliah, M., Ebisuzaki, W., Higgins, W., Janowiak, J., Mo, K.C., Ropelewski, C., Wang, J., Leetma, A., Reynolds, R., Jenne, R. & Joseph, D. (1996). The NCEP/NCAR 40-year Reanalysis Project. *Bulletin of American Meteorological Society*, 77, 437–471.

13. Arthur, A.A. & Jagtap, S.S. (1999). Geographic variation in growing season rainfall during three decades in Nigeria using principal component and cluster analyses. *Theoretical and Applied Climatology*, 63, 107–116.
14. Peng, S. & Fyfe, J. (1996). The coupled patterns between sea level pressure and sea surface temperature in the midlatitude North Atlantic. *Journal of Climate*, 9, 1824–1839.
15. Rasmusson, E.M. & Carpenter, T.H. (1982). Variation in the tropical sea surface temperature and surface wind fields associated with the Southern Oscillation/El Niño. *Monthly Weather Review*, 110, 354–384.
16. Hendon, H.H. (2003). Indonesia rainfall variability: Impacts of ENSO and local air-sea interaction. *Journal of Climate*, 16, 1775–1790.
17. Fu, C., Diaz, H.F. & Fletcher, J.O. (1986). Characteristics of the response of SST in the central Pacific associated with warm episodes of the Southern Oscillation. *Monthly Weather Review*, 114, 1716–1738.
18. Quinn, W., Neal, V.T. & Mayolo, S.E.A. (1987). El Niño occurrences over the past four and a half centuries. *Journal of Geophysical Research*, 92, 14449–14461.
19. Barnett, T.P. (1991). The interaction of multiple time scales in the tropical climate system. *Journal of Climate*, 4, 269–285.
20. Tomita, T. & Yasunari, T. (1993). On the two types of ENSO. *Journal of the Meteorological Society of Japan*, 71(2), 273–283.
21. Ose, T., Song, Y. & Kitoh, A. (1997). Sea surface temperature in the South China Sea – An index for the Asian monsoon and ENSO system. *Journal of the Meteorological Society of Japan*, 75, 1091–1107.